

**Táňa HOLUŠOVÁ<sup>1</sup>, Miguel LOZANO<sup>2</sup>, Alfonso FERNÁNDEZ-CANTELI<sup>3</sup>, Tereza KOMÁRKOVÁ<sup>4</sup>, Dalibor KOCÁB<sup>5</sup>, Stanislav SEITL<sup>6</sup>**

INFLUENCE OF THE GRIPPING FIXTURE ON THE MODIFIED COMPACT TENSION TEST RESULTS: EVALUATION OF THE EXPERIMENTS ON CYLINDRICAL CONCRETE SPECIMENS

**Abstract**

The modified compact tension test (MCT) might become in the future a stable test configuration for the evaluation of fracture-mechanics parameters or also for description of fatigue behavior of composites materials such as concrete. Core drilling is used for sampling of existing structures. These samples have cylindrical shape with the selected thickness to avoid the stress concentration. This contribution focuses on the evaluation of the fracture behavior during static and quasi static tests. Static tests are performed on standard specimen with diameter 150 mm and length 300 mm. The quasi-static tests are performed using two different gripping fixtures. The results for quasi-static tests are represented as L-COD diagrams (i.e. load vs. crack opening displacement) measured on the loading axis. The comparison of results and discussion of advantages and disadvantages are introduced.

**Keywords**

Modified Compact Tension Test, Fracture Parameters, Cementitious Composites, ARAMIS measurement, grips.

**1 INTRODUCTION**

A series of standardized experimental test procedures for evaluation of fracture-mechanics parameters are found in literature, e.g. see [6] and [11]. The two most suitable types of such tests are used for concrete beams with or without reinforcement. In the first case, the three point bending test (3PB) is applied to smaller beams either of dimensions  $40 \times 40 \times 160$  (120) mm<sup>3</sup> or

<sup>1</sup> Ing. Táňa Holušová, Institute of Structural Mechanics, Faculty of Civil Engineering, Brno University of Technology, Veveří 331/95, 602 00 Brno, Czech Republic, phone: (+420) 541 148 209, e-mail: holusova.t@fce.vutbr.cz.

<sup>2</sup> MSc. Miguel Lozano, Dpt. of Construction and Manufacturing Engineering, University of Oviedo, Campus Universitario de Gijón, 33205 Gijón, labresuniovi@gmail.com.

<sup>3</sup> Prof. Alfonso Fernández-Canteli, Dpt. of Construction and Manufacturing Engineering, University of Oviedo, Campus Universitario de Gijón, 33205 Gijón, afc@uniovi.es.

<sup>4</sup> Ing. Tereza Komárková, Institute of Building Testing, Faculty of Civil Engineering, Brno University of Technology, Veveří 331/95, 602 00 Brno, Czech Republic, phone: (+420) 541 147 830, e-mail: komarkova.t@fce.vutbr.cz.

<sup>5</sup> Ing. Dalibor Kocáb, Institute of Building Testing, Faculty of Civil Engineering, Brno University of Technology, Veveří 331/95, 602 00 Brno, Czech Republic, phone: (+420) 541 147 811, e-mail: kocab.d@fce.vutbr.cz.

<sup>6</sup> Doc. Ing. Stanislav Seitl, Ph.D, Institute of Physics of Materials, Academy of Sciences of the Czech Republic, Žitkova 22, 616 62 Brno and Institute of Structural Mechanics, Faculty of Civil Engineering, Brno University of Technology, Veveří 331/95, 602 00 Brno, Czech Republic, phone: (+420) 532 290 361, e-mail: seitl@ipm.cz.

$100 \times 100 \times 400$  (300) mm<sup>3</sup> without reinforcement, see e.g. [2], [6] or [19]. In the second case the four point bend test (4PB) is applied mostly on larger reinforced concrete beams. In both cases the starting notch aims at ensuring localization of the crack growing.

The amount of the material bound to the ligament, defined as the area of the specimen measured from the top of the notch to the back edge of the specimen, is relatively small compared to that of the material used in the fabrication of the 3PB and 4PB tests beams, this representing a relative handicap for this kind of fracture tests. This is the reason why researchers look for another alternative to determine the fracture mechanical properties on more compact specimens, i.e. requiring less material but also being easily obtained from real constructions. With this aim, the wedge splitting test (WST) was postulated [14], which can be applied for measurement of fracture parameters using, indistinctly, cubic (see [7] and [8]) or cylindrical specimens (see [15]). The shape of the modified compact tension specimen comes from the standard compact tension (CT) specimens being used by testing of metallic materials. Different experimental test set-ups have been used as bending test on notched cylindrical halves (semicircular bend, see [3]) but also as disk-shaped compact tension specimens with two holes for placing the pins, see [18]. Another approach for applying the splitting load to the specimen is proposed in [10] where two steel loading frames were applied instead of two holes for pins, although on a cubic shaped CT specimen. Cifuentes et al. recently postulated the study of the applicability of MCT specimen for measuring the fracture energy of concrete that indicates very promising consistency of the specific fracture energy value for different widths and notch depths, were also the comparison of the MCT test with the traditional fracture test 3PB were carried out, see in [2]

The aim of this contribution is to compare the data obtained from standard compression test performed on  $150 \times 300$  mm cylinders in the laboratory of Faculty of Civil Engineering Brno University of Technology with those obtained from the modified compact tension test performed in the laboratory of the University of Oviedo. The MCT specimens have cylindrical shape with diameter 150 mm and thickness 60 mm. The advantages or disadvantages of using eye nuts at the end of the steel bars against the current solution using steel bars directly clamped at the machine grips are also analyzed, see figure 2. The results are summarized as loading diagrams representing the load versus crack opening displacement measured on the axis of the steel bars (Load – COD). The results of the standard pressure test (performed on concrete cylinders) and fracture parameters (calculated from MCT experiments) are also summarized and compared. This contribution continues a previous numerical study performed by finite element software ATENA, see e.g. [1] and [4], focused on the comparison of those two ways of fixing the specimens into the test machine. Obtained fracture-mechanical parameters can be used as input values for modeling in finite element software.

## 2 EXPERIMENT

### 2.1 Material and specimen preparation

Twelve standardized cylinders with 150 mm diameter and 300 mm length were fabricated by the company BETOTECH, ltd. in plain class C 30/37 concrete. The maximum aggregate grain of 4 mm was chosen considering the MCT specimens ligament length. The composition of the concrete mixture is shown in table 1. Six cylinders were sent to the laboratory of University of Oviedo from which four slide specimens with 60 mm thickness were cut off for the MCT tests.

Tab. 1: Composition of used concrete mixture

Designation	CEM I 42,5 R Wet	Ash Opatovice	DTK 0/4 Tovačov	Water	Sika ViscoCrete 20 Gold
Amount [kg]	450	100	1440	250	2

## 2.1 Specimens for standard compression test

The standard compression test was performed on six cylinders after 28 days from the fabrication time for evaluation of the compression strength as the input value for the concrete model to be used in the numerical calculation of the MCT test, see figure 1. Three of those six cylinders were used for evaluation of the static Young modulus according to European standard: EN 12390-13 Testing hardened concrete – Part 13: Determination of secant modulus of elasticity in compression, method B. The measured average dimensions and cylinders weight for evaluating the density are shown in table 2.



Fig. 1: Six standard cylinders prepared for compression test (1-6) and for evaluation of the static Young modulus (4-6)

Tab. 2: Dimensions ( $d$ ,  $l$ ), weights (mass  $m$ ) and densities ( $\rho$ ) of concrete cylinders

Designation	$m$ [kg]	$d$ [mm]	$l$ [mm]	$\rho$ [kg/m <sup>3</sup> ]
1	10.684	149.41	286.43	2127
2	11.001	149.38	292.22	2148
3	10.514	149.37	280.02	2143
4	10.854	149.45	288.27	2146
5	10.870	149.37	289.15	2145
6	10.790	149.38	287.48	2142

## 2.2 Specimen preparation for the modified compact tension test

The shape of the MCT test is based on specimens for standard compact tension test (CT), used for metallic materials [1]. The aim of the present MCT test is to compare different ways of fixing the steel bars to the test machine. The current fixing consists in clamping directly the bars into the grips as seen in figure 2a), which causes rising of an undesirable moment at the ligament due to bending of the bar during the notch opening. Instead, the load can be applied through eye nuts (see figure 2b)) provided just at the bars protruding from the specimen thus allowing a rotation of the specimen during notch opening. This avoids bending of the drawing bars and, as a consequence, the moment at the ligament so that the MCT specimen behavior approaches to that experienced by the CT test. MCT specimens are cut of the prepared cylinders for standard pressure test, but former contributions indicates the convenience of using a plastic pipe of the internal diameter 153 mm, as casting mold, see [2] and [5].

Placing the steel bars into the specimen can be done in two ways. In the first case, the steel bars are placed before concrete casting, so that full connection is achieved between concrete and steel. In the second case, the steel bar must be introduced into specimen after the required 28 days

hardening of concrete. The hole is drilled off from the specimen side for allocating the steel bar, which is then glued by the strong epoxy. The method applied to the MCT test consisting in drilling hole and threading the uncut steel bar through the specimen hole is shown in figure 3. A laser beam on the specimens helps to maintain the right orientation of the drilled hole. The initial notch is machined on the specimen perpendicularly to the steel bar once the epoxy glue gets hard.

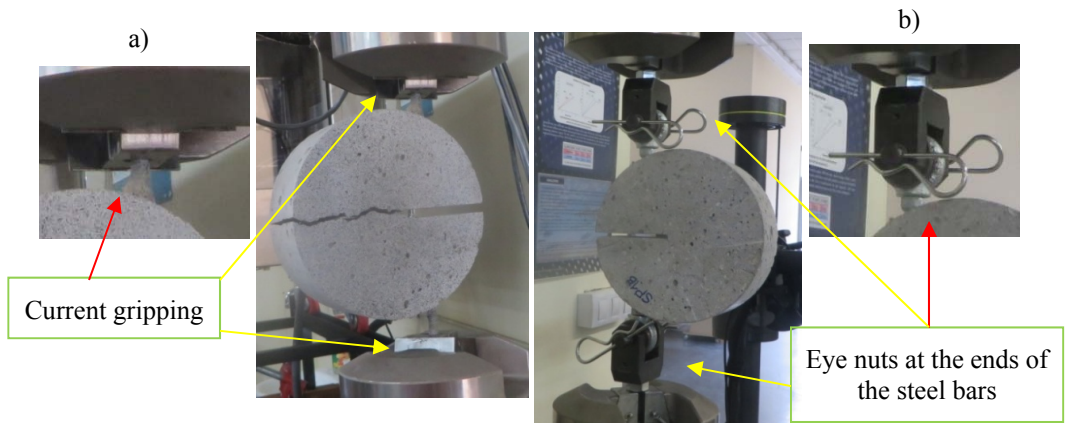


Fig. 2: Fixing of MCT specimen into the test machine: a) Current grips; b) Eye nuts provided at the ends of the steel bars



Fig. 3: Threading the steel bars into the holes drilled in the MCT specimen

### 2.3 MCT test

MCT specimens are marked by the initials SP (specimen), number of specimen and the type of steel bars fixture to the test machine. The current gripping system is denoted by the capital letter A and eye nuts gripping at the ends of the steel bars, by the capital letter B. Five specimens for each fixture system are prepared, the current fixture being denoted SP1A – SP5A and the fixture with eye nuts at the ends of the steel bars, SP1B – SP6B. One extra specimen is used in case of fixture B because specimen SP1B happens to be faulty. All specimens are dimensioned for relative notch

length  $\alpha = 0.3$  and the steel bar placed at a distance  $W = 120$  mm from the back front, while the real measured dimensions are shown in table 3 according the designations in figure 4, where:

- $d$  is the diameter of the specimen in [mm],
- $W$  is the location of the steel bars in [mm],
- $l_{\text{lig}}$  is the length of the ligament  $v$  [mm],
- $a$  is the length of the starting notch measured from the steel bars axis in [mm],
- $B$  is the thickness (breadth) of the specimen in [mm],
- $\alpha$  is the relative notch length [-],
- $A_{\text{lig}}$  is the area of the ligament in [mm<sup>2</sup>].

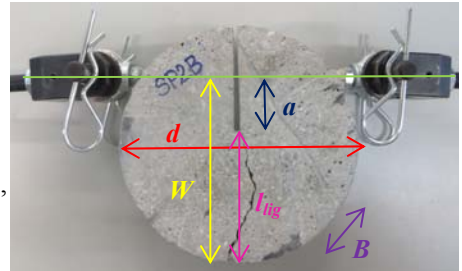


Fig. 4: MCT specimen designations

The ligament area  $A_{\text{lig}}$  is calculated as the product of the ligament length ( $l_{\text{lig}}$ ) times the specimen thickness ( $B$ ). The relative notch length ( $\alpha$ ) is the ratio of the length of the starting notch ( $a$ ) to the parameter of the steel bars location ( $W$ ).

The tests are performed on a servo-hydraulic test machine MTS Bionix of 25 kN loading capacity, see figure 5, meanwhile the surface deformation was captured by the 3D digital image correlation ARAMIS system of GOM, where the preparation of the specimen surface was done according to the recommendation in ARAMIS: User Manual – Software. The speed of the loading was 0.2 mm/min.

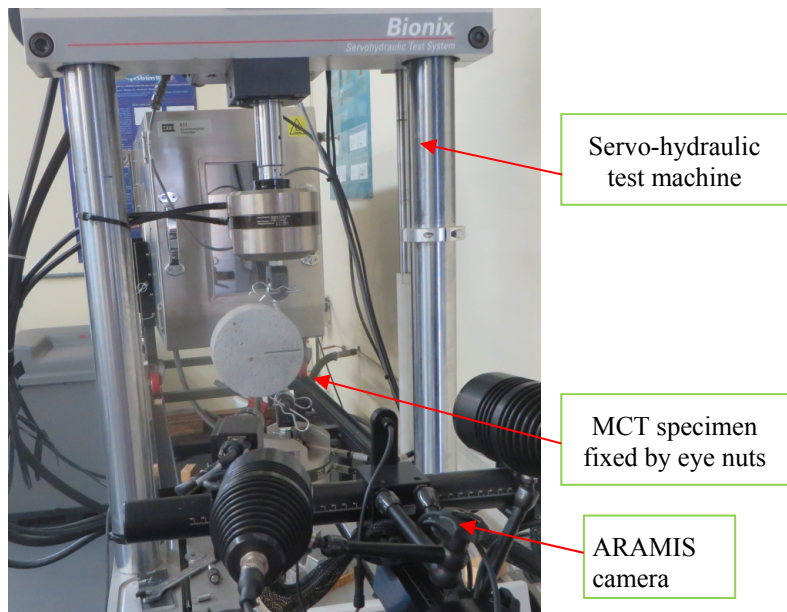


Fig. 5: Servo-hydraulic test machine MTS Bionix with specimen fixed by the eye nuts and 3D optical camera system ARAMIS

Tab. 3: Dimensions of the MCT specimens

Des.	$d$ [mm]	$W$ [mm]	$l_{lig}$ [mm]	$a$ [mm]	$B$ [mm]	$\alpha$ [-]	$A_{lig}$ [mm <sup>2</sup> ]
SP1A	149.72	115	84.50	30.50	60.00	0.265	5070
SP2A	150.00	120	82.55	37.45	59.50	0.312	4912
SP3A	149.70	116	83.58	32.42	60.00	0.279	5015
SP4A	149.10	115	85.60	29.40	57.85	0.256	4952
SP5A	149.10	118	83.50	34.50	58.76	0.292	4906
SP1B	149.60	-	82.20	-	59.00	-	4850
SP2B	149.70	120	83.02	36.98	60.00	0.308	4981
SP3B	149.43	118	83.20	34.80	58.96	0.295	4905
SP4B	149.27	115	84.60	30.40	59.53	0.264	5036
SP5B	149.27	120	85.25	34.75	60.06	0.290	5120
SP6B	149.19	115	84.75	30.25	60.20	0.263	5102

### 3 RESULTS – STANDARD PRESSURE TEST

The standard pressure test was performed on six cylinders with diameter 150 mm and length 300 mm. The speed of the loading was 0.6 MPa/s according to European standard EN 12390-3:2009. Final values of cylindrical strength  $f_{c,cyl}$  and the static modulus of elasticity  $E_{c,s}$  are listed in table 4. Average value of cylindrical strength is  $f_{c,cyl} = 43.8$  MPa which is calculated from the maximum load  $F_{c,max}$  divided by the area of the cylinder's top (calculated from the diameter  $d$  in table 2. The average value of static modulus of elasticity is  $E_{c,s} = 25\ 100$  MPa.

Tab. 4: Final values obtained from pressure test and values of modulus of elasticity

Designation	$F_{c,max}$ [kN]	$f_{c,cyl}$ [MPa]	$E_{c,s}$ [MPa]
1	752.0	42.9	-
2	716.1	40.9	-
3	768.8	43.9	-
4	806.0	45.9	24 100
5	777.4	44.4	26 200
6	785.3	44.8	24 900
$\phi$	-	<b>43.8 ± 1.6</b>	<b>25 100</b>

### 4 RESULTS AND DISCUSSION – MCT TEST

The L-COD (i.e. Load – Crack Opening Displacement) diagram is recording during loading of the MCT specimen measured on the axis of the steel bars, which are used to evaluate the fracture parameters of the material. The loading curves of current fixing (variation A) are shown in the graph in the figure 6 and the loading curve for the second variation (B) are shown in diagram in figure 7.

The results obtained for the specimen with mark SP4B were eliminated from the evaluation because of the bad adjustment of the loading speed during experiment.

#### 4.1 Evaluation of L-COD diagrams

Elastic modulus of elasticity ( $E$ ) was calculated by the recommendation of RILEM [10] from Hook's Law (1) from stress-strain diagram.

$$E = \frac{\sigma}{\varepsilon} \quad (1)$$

The value of fracture toughness  $K_{Ic}$  is calculated by equation (2), where  $P_{max}$  is the maximum achieved load in [N],  $B$  and  $W$  represent the dimensions of the specimen (see table 3),  $Y(\alpha)$  is the shape function for CT specimen as given from [16] and  $B_1(\alpha)$  is the shape function for MCT specimen, taken from [13] and [17].

$$K_{Ic} = \frac{P_{max}}{B \cdot W} \cdot \sqrt{W} \cdot B_1(\alpha) \quad (2)$$

The shape function as given from [16] ( $K_{Ic}^{CT}$ ):

The shape function for place of the steel bar  $W = 110$  mm:

$$Y(\alpha) = 59.139 - 515.78\alpha + 1772.4\alpha^2 - 2591.2\alpha^3 + 1436.6\alpha^4 \quad (3)$$

The shape functions taken from [13] and [17] ( $K_{Ic}^{MCT}$ ):

The shape function for place of the steel bar  $W = 110$  mm:

$$B_1(\alpha) = -23.943 + 309.04\alpha - 1335.2\alpha^2 + 2947.6\alpha^3 - 3202\alpha^4 + 1429.6\alpha^5 \quad (4)$$

The shape function for place of the steel bar  $W = 120$  mm:

$$B_1(\alpha) = -33.482 + 416.97\alpha - 1804.2\alpha^2 + 3948.3\alpha^3 - 4254.7\alpha^4 + 1869.7\alpha^5 \quad (5)$$

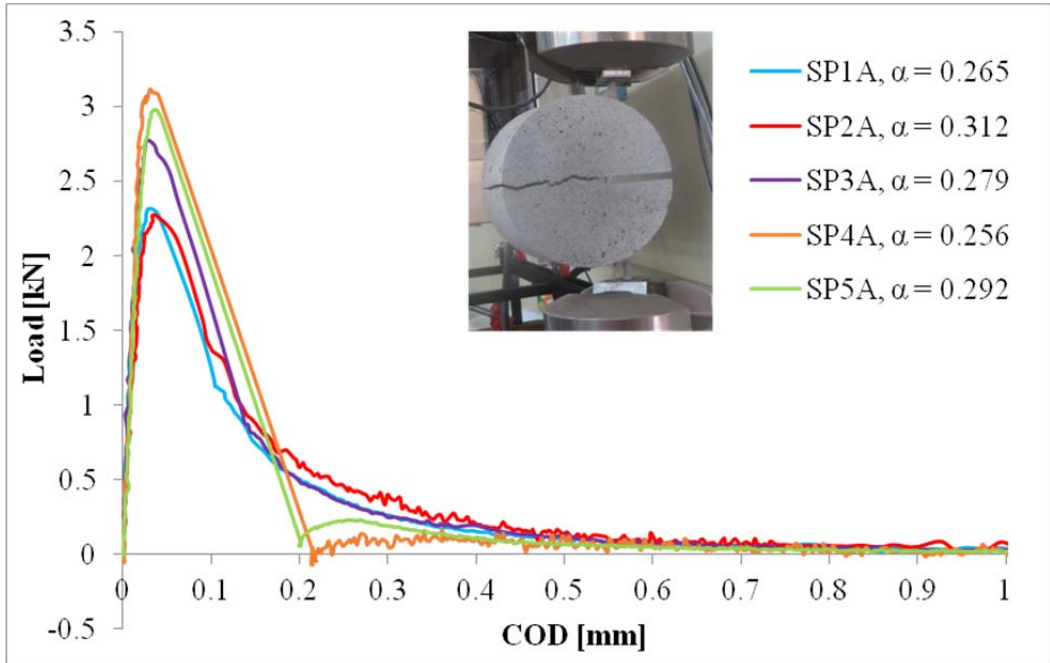


Fig. 6: Loading curves for current variation of fixing of the steel bars (A)

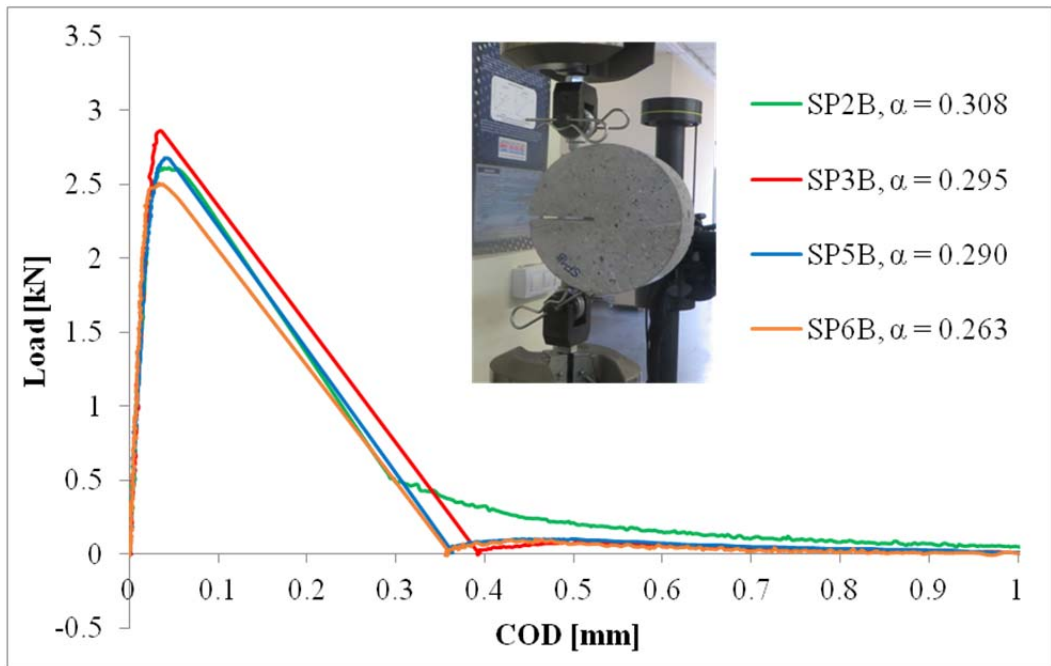


Fig. 7: Loading curves for variation with the use of eye nuts at the ends of the steel bars (B)

The values of fracture energy were calculated by the RILEM recommendation [12]. The value of work of fracture ( $W_f$ ), which corresponds with the area under the loading curve, is divided by the ligament ( $A_{lig}$ ) relevant to exact specimen and loading curve.

Even though all MCT specimen are created from the very same material, the loading curves show in rising part much higher dispersion in case of using the current fixing of the steel bars into test machine (variation A) instead of case with use of eye nuts at the ends of the steel bars (variation B), which can be seen in diagrams in figure 6 and figure 7. The variance of the modulus of elasticity values from the average values is under  $\pm 18\%$  in case of variation A and under  $\pm 5\%$  in case of variation B. However the average values of modulus of elasticity obtained from measured data ( $E$ ) is differed from the average value of modulus of elasticity measured on standard cylinders with dimensions  $150 \times 300$  mm  $E_{c,s} = 25\,100$  MPa under  $\pm 8.2\%$  in case of variation A and under  $\pm 5.1\%$  in case of variation B. The  $E_{c,s}$  value was obtained from standard pressure test on cylinders instead of  $E$  values obtained from tensile tests, so the differences could be expected.

The value of  $K_{Ic}$  was calculated by use of shape function for CT specimen ( $K_{Ic}^{CT}$ ) and for MCT specimen ( $K_{Ic}^{MCT}$ ). In the first case ( $K_{Ic}^{CT}$ ) is the variance of the values under  $\pm 15\%$  in case of variation A and in case of variation B under  $4\%$ . In the second case ( $K_{Ic}^{MCT}$ ) is the variance of the values under  $\pm 12\%$  in case of variation A and in case of variation B under  $9\%$ .

The average value of fracture energy in case of variation A is  $85.58 \pm 9\%$  J/m<sup>2</sup> and in case of variation B is  $140.14 \pm 1\%$  J/m<sup>2</sup>. The process of decreasing part of the loading curve in case of variation B is the reason of  $40\%$  higher value of fracture energy. Approximately two times higher value of crack opening displacement in area of macro-cracks can be seen in loading curves in case of variation B against the case of variation A in figures 6 and 7. This increase is caused by the allowed rotation of the specimen around the pins, which are fitted into eye nuts.

Obtained average values of modulus of elasticity  $E$ , fracture toughness  $K_{Ic}$  (versions CT and MCT) and fracture energy  $G_f$  are shown in table 5 together with their standard deviations.

Tab. 5: Average values of fracture parameters and their standard deviations

Designation	SP_A		SP_B	
	Value	Standard deviation	Value	Standard deviation
$E$ [MPa]	27 343	4 941	23 822	1 099
$K_{Ic}^{CT}$ [MPa $\times$ m <sup>½</sup> ]	0.764	0.116	0.732	0.032
$K_{Ic}^{MCT}$ [MPa $\times$ m <sup>½</sup> ]	0.726	0.090	0.729	0.065
$G_f$ [J/m <sup>2</sup> ]	85.58	7.8	140.14	1.76

## 5 CONCLUSIONS

This contribution is focused on the evaluation of the experimental fracture results obtained by MCT specimens with diameter 150 mm and thickness 60 mm, both for the current fixture represented as steel bars clamped in the grips of the test machine (fixture A) and for the hinged fixture provided by the eye nuts placed at the ends of the steel bars (fixture B), the latter aiming at the configuration of the MCT being most conform with the standard compact tension.

From the measured data the following conclusions are drawn:

- The average values of the Young modulus  $E$  for both fixtures differ from the static Young modulus  $E_{c,s}$  less than 8.2 % in case of fixture A and under 5.1 % in case of fixture B.
- The average values of the fracture toughness parameter  $K_{Ic}^{CT}$  differs for both fixtures less than 4.2 %.
- The average values of the fracture toughness parameter  $K_{Ic}^{MCT}$  for both fixtures differs less than 0.5 %.
- The value of the fracture energy  $G_f$  for fixture B is higher than that for fixture A.

A steep decrease in the decreasing part just behind the top of the loading curve is noticed in the plots of figure 6 and 7. This phenomenon can be observed in both fixture cases. The linear shape of the curves in these areas between 0.05 – 0.3 mm is due to lack of the measured points and the quick descent of the measured load. The rigidity of the test machine and the relatively higher speed of the loading could be, possibly, the reasons of such a phenomenon. However, further study is needed since this effect does not appear in all the cases studied as the graphs confirm.

## ACKNOWLEDGMENT

The paper has been supported by the project of junior specific research with the registration number FAST-J-15-2760 and by the Grant Agency of the Czech Republic number 13-18870 S. The financial support of the project SV-PA-11-012 by the Asturian Regional Government is also acknowledged.

## REFERENCES

- [1] ASTM International Standard E399. Standard test method for linear-elastic method of plane-strain fracture toughness K<sub>Ic</sub> of metallic materials, 2006, 33 pp.
- [2] CERVENKA, V, CERVENKA, J, PUKL, R. ATENA – A tool for engineering analysis of fracture in concrete. Sadhana, Vol. 27, Part 4. 2002, pp. 485–492.
- [3] CIFUENTES, H., LOZANO, M., HOLUŠOVÁ, T., MEDINA, F., SEITL, S., FERNÁNDEZ-CANTELI, A. Applicability of a Modified Compact Tension Specimen for Measuring the Fracture Energy of Concrete. Anales de Mecánica de la Fractura, Vol. 32. 2015, pp. 208–213, ISSN: 0213-3725.

- [4] HASSAN, M. M. Relationship between creep time dependent index and Paris Law parameters for bituminous mixtures. *Journal of the South African Institution of Civil Engineering*, Vol. 55, No. 2. 2013, pp. 8–11, ISSN: 1021-2019.
- [5] HOLUŠOVÁ, T., SEITL, S., CIFUENTES, H., FERNÁNDEZ-CANTELI, A. A numerical study of two different specimen fixtures for the modified compact tension test – their influence on concrete fracture parameters. *Fracture and Structural Integrity*, Vol. 35. 2016, pp. 448–455, (in press).
- [6] HOLUŠOVÁ, T., SEITL, S., FERNÁNDEZ-CANTELI, A., Numerical Simulation of Modified Compact Tension Test depicting of Experimental Measurement by ARAMIS. *Key Engineering Materials*, V. 627. 2014, pp. 277–280, ISSN (web): 1662-9795. doi: 10.4028/www.scientific.net/KEM.627.277.
- [7] KARIHALOO, B. L. *Fracture mechanics and structural concrete*. New York: Longman Scientific & Technical. 1995, 330 pp. ISBN: 978-05-822-1582-5.
- [8] KORTE, S, BOEL, V, DE CORTE, W, DE SCHUTTER, G. Static and fatigue fracture mechanics properties of self-compacting concrete using three-point bending tests and wedge-splitting tests. *Construction and Building Materials*, Vol 57. 2014; pp. 1–8, ISSN: 0950-0618, doi:10.1016/j.conbuildmat.2014.01.090.
- [9] MERTA, I, TSCHEGG, E. K. Fracture energy of natural fibre reinforced concrete. *Construction and Building Materials*, Vol. 40. 2013; pp. 991–997, ISSN: 0950-0618, doi:10.1016/j.conbuildmat.2012.11.060.
- [10] OŽBOLT, J., BOŠNJAK, J., SOLA, E. Dynamic fracture of concrete compact tension specimen: Experimental and numerical study. *Journal of Solids and Structures*, Vol. 50. 2013, pp. 4270–4278, ISSN: 0020-7683, doi: 10.1016/j.jisolstr.2013.08.030.
- [11] RILEM Report 39. Experimental Determination of the Stress-Crack Opening Curve for Concrete in Tension. Technical Committee TC 187. 2007, ISBN: 978-2-35158-049-3.
- [12] RILEM Report 5, *Fracture Mechanics Test Methods for Concrete*, S. P. Shah, A. Carpinteri (Eds.), Hall, London, 1991.
- [13] RILEM TC-50 FMC Recommendation. Determination of the fracture energy of mortar and concrete by means of three-point bend test on notched beams. *Materials & Structures*, Vol. 18, Issue 4. 1985, pp. 287–290, ISSN (web): 1871-6873.
- [14] SEITL, S., VISZLAY, V., CIFUENTES, H., CANTELI, A. Stress analysis of modified compact tension specimens: K-calibration curves. *Transactions of the VŠB – Technical University of Ostrava, Civil Engineering Series*, Vol. 15 No. 2., 2015, (in press).
- [15] TSCHEGG, E. K. Equipment and appropriate specimen shapes for tests to measure fracture values. Austrian Patent Nr. 390328, 1986, Austrian Patent Office.
- [16] VESELÝ, V., HOLUŠOVÁ, T., SEITL, S. Numerical prediction of parasitic energy dissipation in wedge splitting tests on concrete specimens. 18th International Conference Engineering Mechanics 2012, Czech Republic, pp. 1497–1504, ISBN: 978-80-86246-39-0.
- [17] VISZLAY, V., HOLUŠOVÁ, T., Numerická analýza vplyvu modifikácie skúšky excentrickým ťahom na hodnoty súčiniteľov biaxiality. 16th International Conference of PhD Students. 2014, Faculty of Civil Engineering, BUT, CR, pp. 6, CD, ISBN 978-80-214-4851-3.
- [18] VISZLAY, V., Numerická podpora pro analýzu únavového chování cementových kompozitů. 2014, Bachelors thesis, Brno University of technology, Faculty of Civil Engineering, Institute of Structural Mechanics, pp. 44.
- [19] WAGONER, M. P., BUTTLAR, W. G., PULINO, G. H. Disk-shaped Compact Tension Test for Asphalt Concrete Fracture. *Experimental mechanics*, Vol. 45, No. 3. 2005. pp. 270–277. ISSN: 0014-4851, doi: 10.1177/0014485105053205.

- [20] XU, S., REINHARDT, H. W. Determination of double-K criterion for crack propagation in quasi-brittle fracture Part I: experimental investigation of crack propagation. *International Journal of Fracture*, Vol. 98, Issue 2. 1999. pp. 111–149. ISSN (web): 1573-2673, doi: 10.1023/A:1018668929989.

**Reviewers:**

Prof. Jacek Domski, Ph.D., Department of Concrete Structures and Technology of Concrete, Faculty of Civil Engineering, Environmental and Geodetic Sciences, Koszalin University of Technology, Poland.

Ing. Bc. Oldřich Sucharda, Ph.D., Department of Structural Mechanics, Faculty of Civil Engineering, VŠB – Technical University of Ostrava, Czech Republic.